Article

Competitive Influence of Alkali Metals in the Ion Atmosphere on Nucleic Acid Duplex Stability

Published as part of ACS Omega virtual special issue "Nucleic Acids: A 70th Anniversary Celebration of DNA".

Sebastian J. Arteaga, Bruce J. Dolenz, and Brent M. Znosko*

Read Online

ACCESS | Metrics & More | Article Recommendations | Supporting Information

ABSTRACT: The nonspecific atmosphere around nucleic acids, often termed the ion atmosphere, encompasses a collection of weak ion−nucleic acid interactions. Although nonspecific, the ion atmosphere has been shown to influence nucleic acid folding and structural stability. Studies investigating the composition of the ion atmosphere have shown competitive occupancy of the atmosphere between metal ions in the same solution. Many studies have investigated single ion effects on nucleic acid secondary structure stability; however, no comprehensive studies have investigated how the competitive occupancy of mixed ions in the ion atmosphere influences nucleic acid secondary structure stability. Here, six oligonucleotides were optically melted in buffers containing molar quantities, or mixtures, of either XCl (X = Li, K, Rb, or Cs) or NaCl. A correction factor was developed to better predict RNA duplex stability in solutions containing mixed XCl/NaCl. For solutions containing a 1:1 mixture of XCl/NaCl, one alkali metal chloride contributed more to duplex stability than the other. Overall, there was a 54% improvement in predictive capabilities with the correction factor compared with the standard 1.0 M NaCl nearest-neighbor models. This correction factor can be used in models to better predict RNA secondary structure in solutions containing mixed XCl/NaCl.
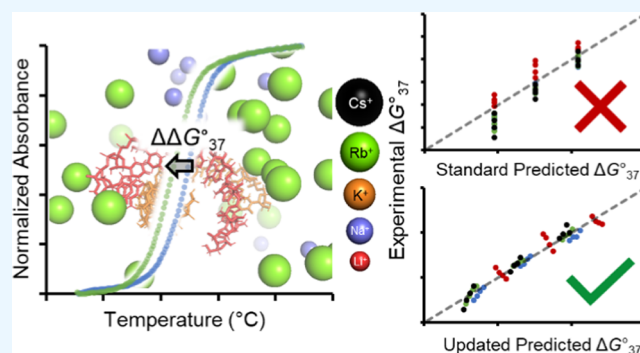
INTRODUCTION

The RNA world hypothesis positions RNA toward the beginning of biological macromolecule development, predating DNA and protein. The presence of rRNA across many biological domains is one of many examples supporting this hypothesis, leading some to think of RNA as a "relic" of the past.[1] This hypothesis expands on the possible environmental conditions and potential functions that RNA could have evolved in and developed.[2−5] Some of these conditions may have included a variety of metal ions,[6,7] extreme pH,[7,8] or extreme temperature.[5]

Many RNA functions that fall outside the central dogma of molecular biology require the presence of metal ions. The ions allow for higher-order folding,[9,10] assist in stabilizing transition states,[11,12] or increase the stability of secondary and tertiary structures.[13−15] Many of the aforementioned phenomena are due to the chemical composition of RNA, which possesses a negative charge at physiological pH. The phosphate groups along the backbone of RNA correspond to one negative charge per group. Therefore, each polynucleotide accumulates a high charge density with each addition of the nucleotide monomer.

The atmosphere surrounding nucleic acids can influence nucleic acid stability and function. Many small molecules and ions occupy this atmosphere and influence the stability of the nucleic acids. Extensive studies have been conducted to investigate the effect that environmental conditions have on nucleic acid stability. Crowding agents have shown to be either stabilizing or destabilizing to nucleic acids, depending on the molecular weight of the crowding agent, functional groups present, and overall percentage of crowding agent in solution.[16−18] These crowding agents have even been shown to have an impact on the efficiency of transcription and translation.[19] Different monovalent,[20−23] divalent,[22,24,25] and some trivalent[26,27] ions in solution have either stabilized or destabilized nucleic acid structures. These conditions can shift the free energy (ΔG°_{37}) and melting temperatures (T_m) of nucleic acids by several kcal/mol and °C, respectively. There are several predictive algorithms and correction factors that have been developed to better predict the secondary structure
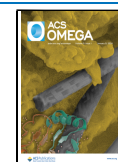
conformation of nucleic acids in solutions containing various metal ions.[21−23,25]

Some nucleic acid secondary structures have specific metal-binding sites, as seen with G-quadruplexes (Figure 1, left). G-
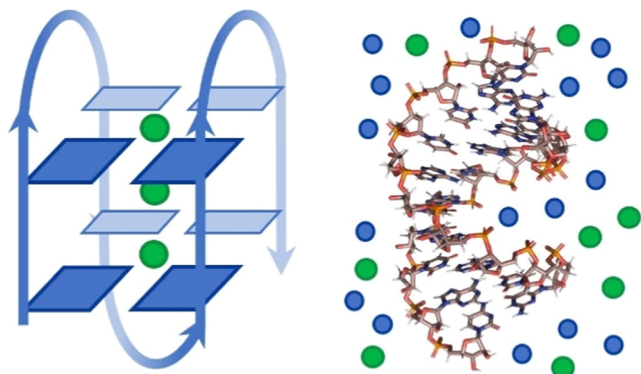

Figure 1. Types of ion−nucleic acid interactions. Chelated ions in a G-quadruplex (left) and the general, nonspecific ion atmosphere surrounding an RNA duplex (right). Blue spheres represent Na^{+} ions, and green spheres represent K^{+} ions.

quadruplexes typically contain monovalent cations (usually K^{+} or Na^{+}) that are chelated in the center of the planar G-quartets, allowing for the formation and stability of the G-quadruplex structure.[28] On the contrary, the general, nonspecific atmosphere around nucleic acids (often termed the "ion atmosphere") encompasses a collection of weak ion−nucleic acid interactions (Figure 1, right).[29−31] These weak interactions can collectively neutralize the high charge density of polynucleotides without direct interaction by minimizing the electrostatic repulsion of each phosphate group.[32] This phenomenon is referred to as screening and often includes interactions between the first hydration layer of a solvated metal ion and the phosphate backbone of a polynucleo-tide.[32−35] The dynamic nature of the ion atmosphere makes studying its composition and its interaction with nucleic acids difficult. Exhaustive and comprehensive methods from the Herschlag lab were developed to identify and quantify the number of ions occupying the ion atmosphere through a method known as ion counting.[36,37] Several other ion counting methods exist, each offering its unique advantages and disadvantages.[38] These methods have been used to uncover differences in ion atmosphere occupancy between nucleic acid types and have provided effective benchmarking data to improve computational methods.[36,39−41]

Computational modeling of direct metal ion interactions with nucleobases has shown ion affinity for specific heteroatoms usually not involved in traditional Watson−Crick−Franklin (WCF) pairing.[42,43] Other computational studies have considered divalent metal ion−backbone interactions for DNA and peptide nucleic acids.[44] Duplexed nucleic acids of eight base pairs or more in the presence of alkali metals have shown competitive occupancy for the ion atmosphere *in silico*.[45−47] With recent advancements in computational studies, a combined implicit and explicit ion placement method has been developed to better mimic the true electrostatic nature of nucleic acids and how they influence the composition of the ion atmosphere.[48] Additionally, computational methods have accurately predicted the composition of the ion atmosphere using molecular dynamic

simulations and Poisson−Boltzmann calculations.[49] The composition of the ion atmosphere around nucleic acids is therefore well characterized by benchtop and *in silico* analysis.

Most ion counting methods investigate the composition of the ion atmosphere without investigating how the composition influences stability. Studies that have investigated ion effects on nucleic acid stability tend to focus on single ion effects with no mixing of metal ions in the same solution.[13,20,21,23,50−53] When studies do investigate mixed ion effects on stability, the studies usually focus on mixed monovalent and divalent ion solutions.[22,54,55] Currently, no comprehensive secondary structure stability analysis of nucleic acids exists with mixed monovalent cationic (alkali metal chloride) solutions; however, native nucleic acids are often found in environments containing more than one monovalent cation.

Na^{+} and K^{+} make up the majority of intracellular monovalent cations.[56] Sodium plays a role in balancing water in the body,[57] transmitting nerve impulses,[58,59] muscle contraction and relaxation,[59] and preventing organ failure.[59,60] Potassium maintains osmotic pressure,[61−63] is used to treat diseases and disorders,[64,65] and helps move nutrients into the cell and waste out of the cell.[66] The sodium−potassium pump controls the cellular concentrations of the two ions and is a well-characterized system that is tightly regulated. Lithium is used in some antipsychotic and hypertension medications,[67,68] and sodium−lithium exchange and sodium−proton exchange are mediated by the same transport system.[69] Rubidium helps in the stimulation of metabolism,[70,71] treats severe heart diseases,[72,73] and is found in muscles.[74,75] Some DNA extraction kits and DNA cloning methods utilize RbCl as a means for enhancing efficacy.[76−78] Cesium shares chemical properties of potassium and can replace potassium in biological systems.[79,80] Although Rb^{+} and Cs^{+} are less biologically relevant, studying the effects of all five monovalent ions on RNA secondary structure stability can assist in understanding the basic trends across the alkali metal ions.

The lack of stability data in this area led to the work here, which aimed to provide preliminary stability data for nucleic acids in solutions containing more than one monovalent cation at different ratios. We compared mixed alkali metal chloride solutions (LiCl, KCl, RbCl, and CsCl) systematically to standard buffer conditions (NaCl) commonly used in traditional optical melting experiments.[81−83] Our findings suggest alkali metal identity is important in stabilizing the nucleic acid secondary structure when in mixed solutions. Some ions appear to have a greater influence on RNA secondary structure stability than others when in the same solution, consistent with the idea of competitive occupancy for ions in the ion atmosphere around nucleic acids.[41,47]

■ MATERIALS AND METHODS

Oligonucleotide Selection and Synthesis. Six oligonu-cleotide duplexes of different lengths and compositions were used in this study, three for RNA and three for DNA. For RNA, the duplexes included the self-complementary oligonu-cleotides 5′-GUAAUAUUAC-3′ and 5′-GAACGUUC-3′, along with the nonself-complementary oligonucleotide 5′-GCUGGC-3′/3′-CGACCG-5′ (referred to as 5′-GCUGGC-3′, herein). The corresponding DNA duplexes contained T in place of U. *RNAstructure*[84−86] software was used to ensure that duplex formation was the most likely secondary structure in a 1.0 M NaCl solution. The second most stable secondary structure predicted was >2.0 kcal/mol less stable than the

desired duplex for each oligonucleotide. Each duplex contained a terminal GC pair to reduce the amount of fraying during optical melting experiments,[87] ensuring a two-state transition. Each synthetic oligonucleotide was purchased from Integrated DNA Technologies, Inc. (Coralville, IA).

Oligonucleotide Purification and Concentration. The purification of oligonucleotides was described in detail previously.[88] In short, the lyophilized oligonucleotides were resuspended in a buffered solution and loaded onto a Sep-Pak C18 Classic Cartridge (Waters) to desalt. After desalting, each sample was loaded onto a thin-layer chromatography (TLC) plate with a fluorescent indicator to separate the desired product from the failure sequences. An additional Sep-Pak cartridge was used following TLC. The absorbance at both 260 and 280 nm for each of the samples was determined in a 1.0 cm cuvette at 80 °C. The concentrations of the single strands were approximated using ε_{260} for the 5′-GUAAUAUUAC-3′, 5′-GTAATATTAC-3′, 5′-GAACGUUC-3′, and 5′-GAACGTTC-3′ duplexes and ε_{280} for the 5′-GCUGGC-3′ and 5′-GCTGGC-3′ duplexes from *RNAcalc*[89,90] software and the Beer−Lambert law.

Buffer Solutions. A total of 17 buffers were made for the analysis of mixed alkali metal effects on nucleic acid duplex stability. Five buffers contained 1.0 M of either LiCl, NaCl, KCl, RbCl, or CsCl with 20.0 mM sodium cacodylate as the buffering agent and 0.5 mM Na$_2$EDTA. The remaining 12 buffers contained either 750 mM XCl/250 mM NaCl, 500 mM XCl/500 mM NaCl, or 250 mM XCl/750 mM NaCl (where X corresponds to either Li, K, Rb, or Cs), 20.0 mM sodium cacodylate, and 0.5 mM Na$_2$EDTA, keeping total the salt concentration at ∼1.0 M. The ratios for each alkali metal chloride mixed with NaCl are referred to as 1:0, 3:1, 1:1, 1:3, and 0:1 herein, where 1:0 refers to 1.0 M XCl/0.0 M NaCl and decreasing amounts of XCl with increasing amounts of NaCl continue as the ratio approaches 0:1.

The buffer for optical melting experiments that is often considered the "standard" melt buffer contains 1.0 M NaCl, 10.0−20.0 mM sodium cacodylate, and 0.5 mM Na$_2$EDTA.[81,91] Duplexes suspended in 1.0 M NaCl, 20.0 mM sodium cacodylate, and 0.5 mM Na$_2$ EDTA were used as reference samples. Each salt mixture was suspended in water and adjusted to a pH of 7.0 with either NH$_4$OH or HCl. All metal chlorides used were ≥99.0% pure.

Optical Melting Studies. A melting scheme of serial dilutions was used to ensure that each duplex was melted at least nine times in each buffer at different concentrations, achieving a ∼50-fold dilution range. Each DNA duplex was melted in one of the five 1.0 M buffers containing a single alkali metal chloride. Each RNA duplex was melted in each of the 17 buffers. Equal mole amounts of each nonself-complementary strand were combined and concentrated to an appropriate volume. All optical melting studies were performed on a Beckman-Coulter DU800 spectrophotometer. The temperature was varied by using an automated high-performance temperature controller. Absorbances for each sample were recorded at both 260 and 280 nm with a ramp rate of 1.0 °C/min and a data acquisition interval of 0.5 °C. The temperature ranged from 10 to 90 °C. Absorbance versus temperature curves were plotted and used to determine thermodynamic parameters.

Thermodynamic Parameter Calculations. For the 5′-GUAAUAUUAC-3′, 5′-GTAATATTAC-3′, 5′-GAACGUUC-3′, and 5′-GAACGTTC-3′ duplexes, the absorbance at 260 nm

versus temperature melt curves were used to determine thermodynamic parameters. For the 5′-GCUGGC-3′ and 5′-GCTGGC-3′ duplexes, the absorbance at 280 nm versus temperature melt curves were used to determine thermodynamic parameters. The raw data from the melt curves was analyzed using *MeltWin*[92] software and fit to an assumed two-state model. The melting temperature (T_m, in kelvin) and oligonucleotide concentrations (C_T, in molar) were used to construct a T_m^{-1} versus $\ln\left(\frac{C_T}{a}\right)$ plot[93] with eq 1[94]

$$\frac{1}{T_m} = \frac{R}{\Delta H°}\ln\frac{C_T}{a} + \frac{\Delta S°}{\Delta H°} \tag{1}$$

where a is 1 for self-complementary sequences and 4 for nonself-complementary sequences, and R is the gas constant 1.987 cal K^{-1} mol^{-1}. The enthalpy ($\Delta H°$) and entropy ($\Delta S°$) of the system were determined by the slope and intercept of the plot. The Gibb's free energy at 37 °C ($\Delta G°_{37}$) was calculated using eq 2

$$\Delta G°_{37} = \Delta H° - (310.15\ K)\Delta S° \tag{2}$$

Only the parameters derived from the T_m^{-1} versus $\ln\left(\frac{C_T}{a}\right)$ plot were used in comparisons between standard buffer and/or predicted values using the standard 1.0 M NaCl nearest-neighbor (NN) model for predicting RNA duplex stability.[81,91,95] Errors reported for the averages of fittings and van't Hoff plots are average relative sample standard deviations calculated by *MeltWin*.[92]

Thermodynamic Parameter Comparisons. All thermodynamic parameters for duplexes in 1.0 M XCl and mixed solutions were compared to parameters derived from duplexes in a standard melt buffer. The $\Delta\Delta G°_{37}$ values for duplexes in XCl-containing buffers compared to standard melt buffer were calculated using eq 3

$$\Delta\Delta G°_{37} = \Delta G°_{37,1.0\,M\,NaCl} - \Delta G°_{37,XCl} \tag{3}$$

where $\Delta G°_{37,1.0\,M\,NaCl}$ is equal to the free energy of duplex formation in the standard 1.0 M NaCl melt buffer and $\Delta G°_{37,XCl}$ is the free energy in each of the mixed alkali metal chloride solutions (ratios of 1:0, 3:1, 1:1, and 1:3).

The average deviation in $\Delta G°_{37}$ ($\Delta\Delta G°_{37,ave}$) from standard melt buffer for duplexes in alkali metal solutions containing XCl was calculated for each duplex using eq 4

$$\Delta\Delta G°_{37,ave} = \frac{\sum \left(\Delta G°_{37,1.0\,M\,NaCl} - \Delta G°_{37,XCl}\right)}{4} \tag{4}$$

The $\Delta\Delta G°_{37,competition}$ for each duplex in each XCl buffer was calculated using eq 5

$$\Delta\Delta G°_{37,competition} = |\Delta G°_{37,1:1} - \Delta G°_{37,pure}| \tag{5}$$

where $\Delta G°_{37,1:1}$ represents the free energy of duplex formation for duplexes in 1:1 solutions of XCl/NaCl, and $\Delta G°_{37,pure}$ represents the free energy in a 1.0 M solution of NaCl or XCl. Errors associated with $\Delta\Delta G°_{37}$, $\Delta\Delta H°$, and $\Delta\Delta S°$ were propagated from average relative sample standard deviations using standard error propagation calculations. Similar equations were used for $\Delta H°$ and $\Delta S°$ comparisons (eqs S1−S6).

Derivation of Proposed Correction Factor for Duplexes in Mixed Alkali Metal Chloride Solutions. A variety of correction factors to the standard 1.0 M NaCl NN model[95] were tested. The following were used as variables:
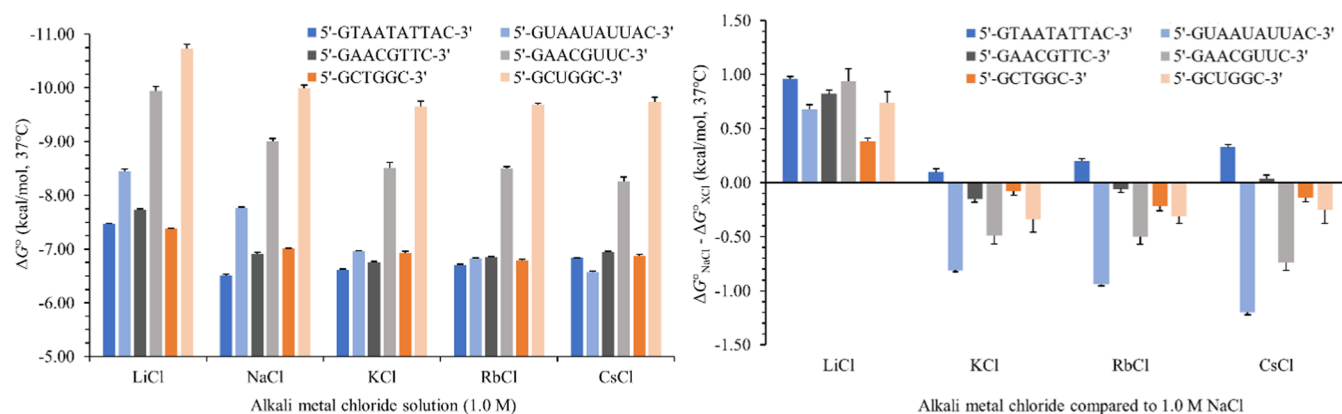
Figure 2. Free energy change ($\Delta G°_{37}$) for duplex formation in various alkali metal chloride buffers. The $\Delta G°_{37}$ (left) and the $\Delta\Delta G°_{37}$ (calculated using eq 3) for 1.0 M XCl (X = Li, K, Rb, or Cs) compared to 1.0 M NaCl (right) for the 5′-GUAAUAUUAC-3′ (0.20 f_{GC}), 5′-GTAATATTAC-3′ (0.20 f_{GC}), 5′-GAACGUUC-3′ (0.50 f_{GC}), 5′-GAACGTTC-3′ (0.50 f_{GC}), 5′-GCUGGC-3′ (0.83 f_{GC}), and 5′-GCTGGC-3′ (0.83 f_{GC}) duplexes are depicted. Each oligonucleotide forms a duplex in solution with its complement. The DNA duplexes are depicted by the darker shade of each color and contain Ts. The RNA duplexes are depicted by the lighter shade of each color and contain Us. Positive $\Delta\Delta G°_{37}$ values indicate a stabilizing effect from XCl compared to NaCl, and negative $\Delta\Delta G°_{37}$ values indicate a destabilizing effect.

ionic radius of alkali metal (R_i), concentration of alkali metal chloride and sodium chloride ([XCl] and [NaCl], respectively), and fraction of GC pairs in the duplex (f_{GC}). Linear regression was used to derive the correction factors, assuming independent linear relationships between each of the parameters and stability of duplexes. Data from all 16 buffers (excluding the 0:1 buffer) for each of the duplexes were used in the fitting procedure. The coefficients derived from the linear regression were validated with a leave-one-out analysis, similar to what was conducted previously (see the Supporting Materials and Methods).[96]

RESULTS

DNA and RNA with Alkali Metals. Both DNA and RNA contain negatively charged phosphate groups at physiological pH, causing both molecules to have high charge densities. Although similar in structure, duplexed RNA has been shown to have a higher electrostatic potential when compared to duplexed DNA.[41,97] This higher electrostatic potential is a proposed reason for stronger interactions with ions in the ion atmosphere.[41,98,99] Optical melting experiments of three RNA duplexes and their three DNA equivalents revealed that RNA is also more stable than DNA in electrolytic conditions (Figure 2). The raw thermodynamic parameters for nucleic acid duplexes in each of the molar alkali metal solutions are provided in the Supporting Information (Tables S1 and S2). Example melt curves for duplexes in each of the 1.0 M buffers can be found in the Supporting Information (Figure S1). All melt curves exhibited a single sigmoidal transition, which is suggestive of two-state melting.

DNA and RNA in Pure Alkali Metal Chloride Solutions. Each RNA duplex had a more negative $\Delta G°_{37}$ compared to that of its equivalent DNA duplex in each of the pure 1.0 M buffers (Figure 2, left). This finding is consistent with previous findings that reported that RNA duplexes are more thermodynamically stable than their DNA counterparts.[100−104] One exception was seen with the 5′-GUAAUAUUAC-3′ and 5′-GTAATATTAC-3′ duplexes in 1.0 M CsCl, where the 5′-GTAATATTAC-3′ duplex had a more negative $\Delta G°_{37}$ (Figure 2, left). The difference in stability between the RNA and its DNA equivalent also varied the least for the 5′-GUAAUAUUAC-3′ and 5′-GTAATATTAC-3′

duplexes, with the $\Delta G°_{37}$ in 1.0 M RbCl being within 0.12 kcal/mol between the two nucleic acid types (Figure 2, left). The 5′-GAACGTTC-3′ and 5′-GAACGUUC-3′ duplexes had the largest difference in $\Delta G°_{37}$ between RNA and DNA in 1.0 M LiCl, and the smallest difference in $\Delta G°_{37}$ in the 1.0 M CsCl buffer, 2.21 and 1.31 kcal/mol, respectively (Figure 2, left). The 5′-GCUGGC-3′ and 5′-GCTGGC-3′ duplexes varied the most in $\Delta G°_{37}$ between the RNA and DNA nucleic acid types in pure 1.0 M buffers (Figure 2, left). The largest difference in $\Delta G°_{37}$ in this study, 3.34 kcal/mol, was between the 5′-GCUGGC-3′ and 5′-GCTGGC-3′ duplexes in the 1.0 M LiCl solution (Figure 2, left).

When comparing the stability of nucleic acids in 1.0 M XCl versus 1.0 M NaCl, the 5′-GTAATATTAC-3′ duplex was always less stable in 1.0 M NaCl, a feature unique to this duplex, indicated by all positive values in Figure 2 (right). Consistent with previous studies,[14,15] all RNA and DNA oligonucleotides were more stable in 1.0 M LiCl than in 1.0 M NaCl (Figure 2, right). The 5′-GUAAUAUUAC-3′, 5′-GAACGUUC-3′, 5′-GAACGTTC-3′, 5′-GCUGGC-3′, and 5′-GCTGGC-3′ duplexes were all less stable in 1.0 M KCl, RbCl, and CsCl than in 1.0 M NaCl (Figure 2, right). The largest difference in stability between 1.0 M XCl and 1.0 M NaCl was seen for the 5′-GUAAUAUUAC-3′ duplex in 1.0 M CsCl, which was 1.20 kcal/mol less stable than that in 1.0 M NaCl (Figure 2, right). The smallest differences between 1.0 M XCl and 1.0 M NaCl were for the 5′-GAACGTTC-3′ duplex in 1.0 M RbCl (0.06 kcal/mol less stable than that in 1.0 M NaCl) and in 1.0 M CsCl (0.04 kcal/mol more stable than that in 1.0 M NaCl) (Figure 2, right). The difference between 1.0 M XCl and 1.0 M NaCl was greater for RNA compared to DNA regardless of sequence or length. The stability of the 5′-GUAAUAUUAC-3′ duplex in different alkali metal solutions exhibited a clear trend of decreasing stability with increasing ionic radius. The 5′-GAACGUUC-3′ duplex had a similar trend with KCl and RbCl being close in value (−0.49 and −0.50 kcal/mol, respectively) (Figure 2, right). All other duplexes displayed no notable trends.

RNA in Mixed Alkali Metal Chloride Solutions. The raw thermodynamic data for each RNA duplex in mixed solutions can be found in the Supporting Information (Table S2). RNA duplexes in solutions containing LiCl were more
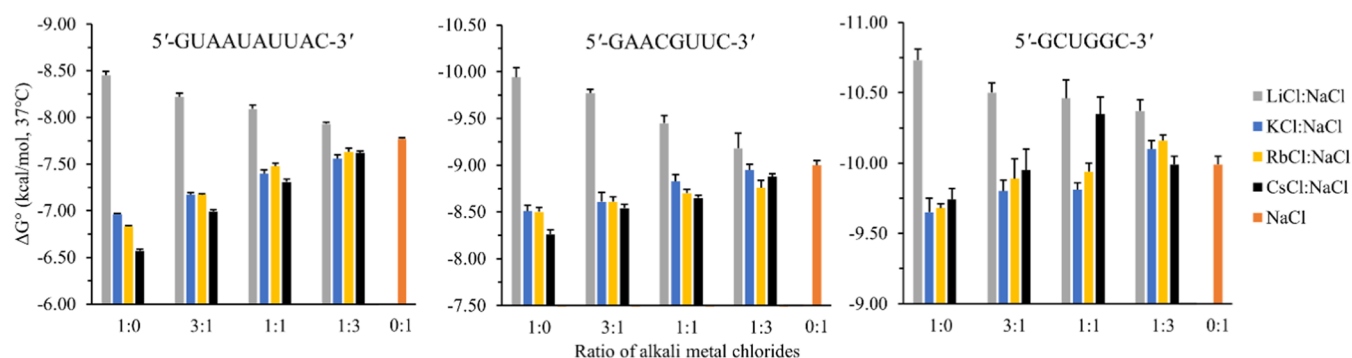
Figure 3. Free energy change (ΔG°_{37}) for RNA duplex formation in various mixed alkali metal chloride solutions. The three RNA duplexes, 5′-GUAAUAUUAC-3′ $(0.20\ f_{GC}$, left), 5′-GAACGUUC-3′ $(0.50\ f_{GC}$, middle), and 5′-GCUGGC-3′ $(0.83\ f_{GC}$, right), were optically melted in each of the 17 alkali metal chloride buffers. All XCl (X = Li, K, Rb, or Cs) were mixed with NaCl at specific ratios that are outlined in the Materials and Methods section. Note that the range on the y-axis is different for each panel.

Table 1. Differences in ΔG°_{37} for RNA Duplexes in Alkali Metal Solutions Compared with Standard Buffer Conditions

sequence (5′−3′)[b]	f_{GC}[c]	ratio (XCl/NaCl)[d]	$\Delta\Delta G^\circ_{37}$ (kcal/mol) for alkali metal solutions (X)[a]			
			Li	K	Rb	Cs
GUAAUAUU-AC	0.20	1:0	0.68 ± 0.04	−0.81 ± 0.01	−0.94 ± 0.01	−1.20 ± 0.02
		3:1	0.45 ± 0.04	−0.60 ± 0.02	−0.60 ± 0.01	−0.78 ± 0.02
		1:1	0.32 ± 0.04	−0.37 ± 0.04	−0.29 ± 0.03	−0.46 ± 0.03
		1:3	0.16 ± 0.02	−0.21 ± 0.04	−0.14 ± 0.04	−0.15 ± 0.02
		$\Delta\Delta G^\circ_{37,ave}$[e]	0.40 ± 0.02	−0.50 ± 0.02	−0.49 ± 0.02	−0.65 ± 0.02
GAACGUUC	0.50	1:0	0.94 ± 0.11	−0.49 ± 0.08	−0.50 ± 0.07	−0.74 ± 0.07
		3:1	0.77 ± 0.06	−0.39 ± 0.11	−0.39 ± 0.07	−0.46 ± 0.06
		1:1	0.45 ± 0.09	−0.17 ± 0.09	−0.30 ± 0.06	−0.35 ± 0.06
		1:3	0.18 ± 0.17	−0.05 ± 0.08	−0.24 ± 0.09	−0.12 ± 0.06
		$\Delta\Delta G^\circ_{37,ave}$[e]	0.59 ± 0.06	−0.28 ± 0.05	−0.36 ± 0.04	−0.42 ± 0.03
GCUGGC	0.83	1:0	0.74 ± 0.10	−0.34 ± 0.12	−0.31 ± 0.07	−0.25 ± 0.10
		3:1	0.51 ± 0.09	−0.19 ± 0.10	−0.10 ± 0.15	−0.04 ± 0.16
		1:1	0.47 ± 0.14	−0.18 ± 0.08	−0.05 ± 0.08	0.36 ± 0.13
		1:3	0.38 ± 0.10	0.11 ± 0.08	0.17 ± 0.07	0.00 ± 0.08
		$\Delta\Delta G^\circ_{37,ave}$[e]	0.53 ± 0.08	−0.15 ± 0.08	−0.07 ± 0.08	0.02 ± 0.09
		Overall $\Delta\Delta G^\circ_{37,ave}$	0.50	−0.31	−0.31	−0.35

[a]Values were calculated using eq 3. [b]Oligonucleotides form duplexes in solution with their complement. [c]The fraction of GC pairs in the duplex. [d]Concentrations associated with the ratios can be found in the Materials and Methods section. [e]Values were calculated using eq 4, and propagated standard deviations were derived from experimental uncertainty.

stable than RNA duplexes in all of the other mixtures (Figure 3). In general, as the concentration of NaCl in the buffers increased, the ΔG°_{37} of the duplexes in mixed buffered solutions converged toward the ΔG°_{37} of the duplexes in 1.0 M NaCl. An exception to this trend was for the 5′-GCUGGC-3′ duplex in 1:1 and 1:3 solutions. The ΔG°_{37} in the 1:1 solution for the 5′-GCUGGC-3′ duplex containing CsCl/NaCl was more negative than that in the 1:3 solution (Figure 3, right). The 5′-GCUGGC-3′ duplex was also more stable in all of the 1:3 mixtures than in 1.0 M NaCl.

When considering similar plots with ΔH° and ΔS°, there were no observable trends (Figures S2−S5). The cause for no notable trend may be due to the entropy−enthalpy compensation phenomenon. However, due to the large errors associated with ΔH° and ΔS°, this not a definitive explanation and would require additional rigorous testing to validate.[105−107]

The theoretical dielectric constants for each alkali metal chloride solution were calculated according to eqs S7 and S8 and can be found in Tables S3 and S4. Each of the mixed solutions had calculated dielectric constants within 1.0 unit of each other (Table S4). The LiCl- and CsCl-containing samples had the same calculated constants (Tables S3 and S4). This suggests that dielectric constants of the solution may not play a role in the stability of duplexes.

Comparing $\Delta\Delta G^\circ_{37}$ of RNA in Mixed Alkali Metal Chloride Solutions. The $\Delta\Delta G^\circ_{37,ave}$ for each alkali metal solution compared to standard buffer conditions of 1.0 M NaCl was calculated using eq 4. The 5′-GUAAUAUUAC-3′ duplex had a similar average difference in ΔG°_{37} in the KCl and RbCl solutions compared to the 1.0 M NaCl standard buffer conditions, −0.50 and −0.49 kcal/mol, respectively (Table 1). For the 5′-GUAAUAUUAC-3′ duplex in the LiCl solutions, the ΔG°_{37} deviated the least from 1.0 M NaCl with a $\Delta\Delta G^\circ_{37,ave}$ of 0.40 kcal/mol, stabilizing compared to 1.0 M NaCl (Table 1). The same duplex in the CsCl solutions had the largest deviation from 1.0 M NaCl with a $\Delta\Delta G^\circ_{37,ave}$ of −0.65 kcal/mol, destabilizing in comparison to 1.0 M NaCl (Table 1). The 5′-GCUGGC-3′ duplex in the KCl, RbCl, and CsCl solutions was least affected by a change in buffer,
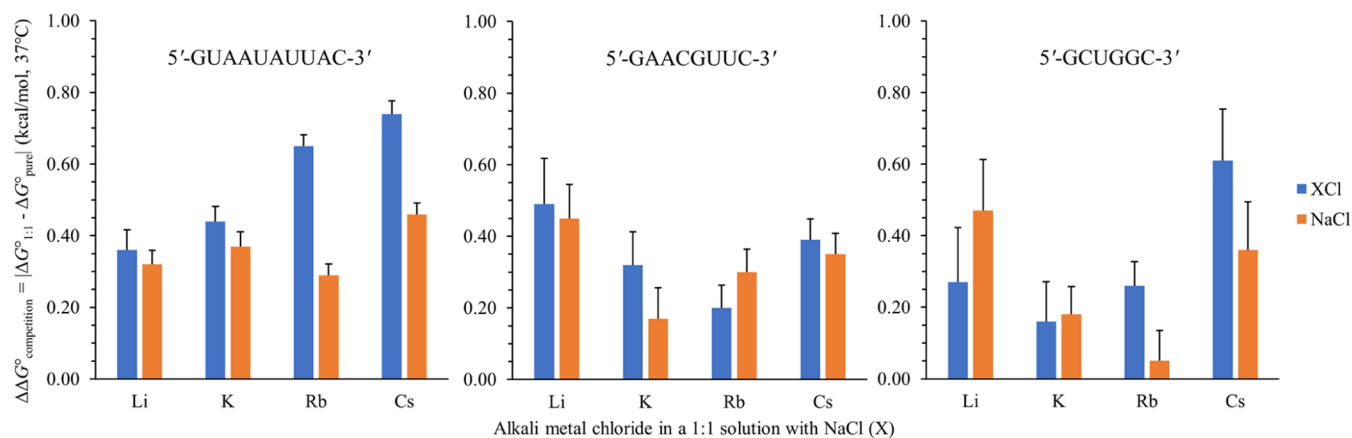
Figure 4. $\Delta\Delta G^\circ_{37,\text{competition}}$ (calculated using eq 5) for RNA duplexes in 1:1 XCl/NaCl solutions (X = Li, K, Rb, or Cs) compared to pure alkali metal chloride solutions. $\Delta\Delta G^\circ_{37,\text{competition}}$ for the 5′-GUAAUAUUAC-3′ (0.20 f_{GC}, left), 5′-GAACGUUC-3′ (0.50 f_{GC}, middle), and 5′-GCUGGC-3′ (0.83 f_{GC}, right) duplexes is on the y-axis. Each pair of bars represents an oligonucleotide in mixed solutions of XCl with NaCl. The blue bars represent the comparison between the 1:1 XCl/NaCl solution and the 1:0 XCl solution, with the X corresponding to the alkali metal depicted on the x-axis. The orange bars represent the comparison between the same 1:1 XCl/NaCl solutions and the 0:1 NaCl solution. For each pair of bars, the alkali metal chloride with a $\Delta\Delta G^\circ_{37,\text{competition}}$ value closer to zero had more influence on RNA duplex stability when in mixed solutions with the other alkali metal chloride.

exhibiting $\Delta\Delta G^\circ_{37,\text{ave}}$ values of −0.15, −0.07, and 0.02 kcal/mol, respectively (Table 1). The 5′-GCUGGC-3′ and 5′-GAACGUUC-3′ duplexes were most affected by the presence of LiCl in solution, exhibiting a $\Delta\Delta G^\circ_{37,\text{ave}}$ of 0.59 and 0.53 kcal/mol, respectively, stabilizing compared to 1.0 M NaCl (Table 1). The Li-containing solutions were always stabilizing compared to NaCl. The K-, Rb-, and Cs-containing solutions were mostly destabilizing compared to NaCl. The overall $\Delta\Delta G^\circ_{37,\text{ave}}$ deviation from 1.0 M NaCl standard buffer for Li⁺, K⁺, Rb⁺, and Cs⁺ solutions from most stabilizing to most destabilizing is Li⁺ > Cs⁺ > K⁺ ≈ Rb⁺, with the Li⁺ solutions being stabilizing and the other solutions being destabilizing compared to Na⁺.

$\Delta\Delta G^\circ_{37,\text{competition}}$ for Alkali Metals. $\Delta\Delta G^\circ_{37,\text{competition}}$ is a metric for determining how much a single metal ion influences the stability of a nucleic acid when mixed in solutions containing other metal ions. The lower the value for $\Delta\Delta G^\circ_{37,\text{competition}}$, the closer the measured ΔG°_{37} was to the ΔG°_{37} of the nucleic acid in a pure solution of monovalent cations. As an example, if the calculated $\Delta\Delta G^\circ_{37,\text{competition}}$ of a nucleic acid in a mixed LiCl/NaCl solution was 0.16 for Li⁺ and 0.45 for Na⁺, Li⁺ could be said to have more of an influence on the stability of the nucleic acid when in a 1:1 mixed solution with Na⁺. This is because the ΔG°_{37} of the nucleic acid in 1:0 LiCl was closer to the ΔG°_{37} of the nucleic acid in 1:1 LiCl/NaCl compared to the ΔG°_{37} of the nucleic acid in 0:1 NaCl. Therefore, a lower $\Delta\Delta G^\circ_{37,\text{competition}}$ value would correspond to a cation that has a greater influence on the stability of the nucleic acid sample in mixed solutions. For the 5′-GUAAUAUUAC-3′, 5′-GAACGUUC-3′, and 5′-GCUGGC-3′ RNA duplexes, the $\Delta\Delta G^\circ_{37,\text{competition}}$ values for Li⁺ and K⁺ were about the same as Na⁺ in each solution, within propagated experimental uncertainty (Figure 4). These findings suggested that when Li⁺ and Na⁺ or K⁺ and Na⁺ are in solution with one another, the stability of the nucleic acid in solution is equally influenced by either ion. The $\Delta\Delta G^\circ_{37,\text{competition}}$ for the 5′-GUAAUAUUAC-3′ and 5′-GCUGGC-3′ duplexes in solutions containing Rb⁺ and Na⁺ or Cs⁺ and Na⁺ suggested that Na⁺ had a greater influence on

the overall stability of nucleic acids in those solutions (Figure 4). The 5′-GAACGUUC-3′ duplex showed no such trends.

Predicting RNA Duplex Stability in Mixed Alkali Metal Chloride Solutions. Correction factors to the standard 1.0 M NaCl RNA NN parameters that account for varying concentrations of individual metal cations (Na⁺ only and Mg²⁺ only) have previously been reported.[23,96] No correction factors exist for predicting the stability of RNA duplexes in solutions containing a mixture of monovalent ions. The data reported here was used to derive such a correction factor. The following correction factor to be used for RNA duplexes in mixed alkali metal chloride solutions with NaCl is

$$\Delta G^\circ_{37}(2) = \Delta G^\circ_{37}(1) + 0.777R_i - 0.411[\text{XCl}]$$
$$- 0.513f_{GC} - 0.782[\text{NaCl}] \quad (6)$$

where $\Delta G^\circ_{37}(2)$ is the predicted ΔG°_{37} in kcal/mol for a mixed alkali metal chloride solution, $\Delta G^\circ_{37}(1)$ is the predicted ΔG°_{37} in kcal/mol using the standard 1.0 M NaCl NN parameters,[95] R_i is the ionic radius in Å[108] of the alkali metal mixed with NaCl in solution (values for ionic radii used can be found in Table S5), [XCl] is the concentration of the alkali metal chloride in M, and f_{GC} is the fraction of GC pairs in the duplex. A leave-one-out analysis validated the chosen coefficients in eq 6 (Figure S6 and Table S6).

Equation 6 was used to predict the ΔG°_{37} of duplex formation for all 48 oligonucleotide samples in alkali metal chloride buffers other than 1.0 M NaCl. Plotting experimental ΔG°_{37} versus predicted ΔG°_{37} resulted in an R^2 value of 0.953 and a line-of-best-fit with a slope of 1.001 and a y-intercept of 0.008 (Figure 5). The experimental ΔG°_{37} versus predicted ΔG°_{37} values using the standard NN parameters[95] with no correction factor (Figure S7) and the percent improvement for the predicted ΔG°_{37} of various categories (Table S7) can be found in the Supporting Information.

■ **DISCUSSION**

Nucleic Acids in Solutions with Alkali Metals. The electrostatic repulsion of the phosphate backbone is neutralized by ions in the ion atmosphere, allowing for the folding of
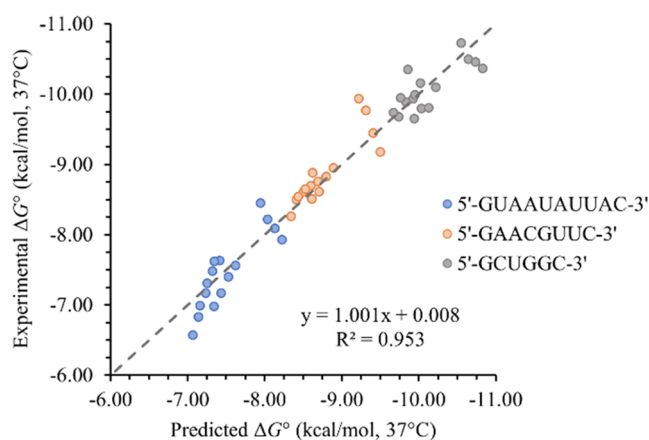
Figure 5. Experimental $\Delta G°_{37}$ versus predicted $\Delta G°_{37}$ using eq 6. The dashed line represents the ideal predictive model that exactly predicts the experimental results. The linear equation and R^2 value are for the plotted data. An optimal slope and y-intercept would be 1.000 and 0.000, respectively, with an R^2 of 1.000 to signify the accurate predictive capabilities of eq 6.

nucleic acids. Lithium chloride has been shown to stabilize duplexed regions of nucleic acids[15] while destabilizing more intricate secondary structures such as G-quadruplexes.[109] The findings here were consistent with previous studies, with LiCl stabilizing duplexed nucleic acids. The Li$^+$ ion has the highest charge density of the ions studied here. Some studies postulate that increased charge density of ions leads to increased stability of dsRNA.[110] The Li$^+$ ion has also been shown to increase the stability of a glycine residue *in silico* due to an increase in water density around the carboxylate group of the residue and the presence of the first hydration shell of the Li$^+$ ion, a feature unique to this ion compared to other alkali metal ions.[111] In this study, the ion with the highest charge density was the most stabilizing, and the ion with the lowest charge density was often the most destabilizing to nucleic acid duplexes.

Previous studies also suggested that the identity of alkali metal ions in solution with a nucleic acid sample did not affect secondary structure stability for alkali metal ions Na$^+$, K$^+$, Rb$^+$, and Cs$^+$.[15] Additional studies investigating the composition of the ion atmosphere have shown slight preferential occupancy of specific ions in the atmosphere, depending on the nucleic acid type.[36,41] The data reported here show that there is not only a measurable difference in stability for nucleic acid duplexes in various alkali metal chloride-containing solutions, but the difference in stability could be dependent on the fraction of GC (f_{GC}) pairs in the duplexes. The reason for the inclusion of the f_{GC} variable in eq 6 is discussed below.

$\Delta G°_{37}$ also varied between nucleic acid types of the same sequence in various alkali metal chloride solutions (Figure 2). It is well-known that standard A-form RNA has a slightly larger charge density than standard B-form DNA along the minor groove.[41,97,112] This difference in charge density is one possible explanation for the increased association of ions with RNA duplexes compared to DNA duplexes.[41] $\Delta G°_{37}$ values for RNA duplexes were substantially more affected by ion identity compared to the DNA duplexes (Figure 2, right). One reason for this could be due to the slight preferential association of ions to RNA over DNA. The additional ions could stabilize the RNA duplexes more than the DNA duplexes. Although the $\Delta G°_{37}$ values for the 5′-GUAAUAUUAC-3′ and 5′-GTAA-TATTAC-3′ duplexes were similar for alkali metals K, Rb, and

Cs (Figure 2, left), comparing $\Delta G°_{37}$ to the 1.0 M NaCl standard buffer solution resulted in notable differences for the RNA-oligonucleotide (>0.50 kcal/mol) while the DNA-oligonucleotide stayed within 0.50 kcal/mol (Figure 2, right).

Due to the similarities between the dielectric constants for the mixed alkali metal chloride solutions (Table S4), the dielectric constant of solutions likely does not play a role in the stabilization of duplexes. An additional variable to consider is the ionic radius of the metal ions. With the dynamic nature of the hydration shell surrounding a dissociated monovalent ion,[35] the radii for consideration are often difficult to determine. Many researchers have used different values for ionic radii in their comparisons and calculations. Some have used the fully dehydrated ionic radii,[14] while others have used variations of coordinated ions[108] with varying degrees of hydration.[15,36,39,40,98,110,113,114] Many studies have suggested that ionic radii are necessary to consider when comparing nucleic acid stability or competitive ion binding in different solutions[46,110,115] while others suggest no such comparison is necessary.[13,40,116] In this work, the ionic radius for each of the alkali metals had a linear relationship with the destabilization of RNA duplexes (Figure S8) and was, therefore, used as a variable in the correction factor.

Another variable that is frequently considered when developing correction factors to the standard 1.0 M NaCl nearest-neighbor model is f_{GC}. Studies reporting correction factors for the effects of [Na$^+$] on RNA[23] and DNA duplex stability,[21,117] correction factors for the effects of [Mg^{2+}] on RNA[96] and DNA duplex stability,[22] and nearest-neighbor parameters for RNA duplexes in crowding conditions[16] all used f_{GC} as a variable. As a result, f_{GC} was tested as a parameter here, and its inclusion resulted in an improved prediction accuracy.

Competitive Occupancy of the Ion Atmosphere and $\Delta G°_{37}$. Monovalent cations have been found to preferentially occupy the ion atmosphere when in mixed solutions.[36,45,46] The measured $\Delta G°_{37}$ values of nucleic acids in mixed ionic solutions suggested that preferential occupancy affects the stability of duplexed nucleic acids. The Na$^+$ ion appeared to influence secondary structure stability for the 5′-GUAAUAUUAC-3′ and the 5′-GCUGGC-3′ duplexes more than the Rb$^+$ or Cs$^+$ ions when in a 1:1 mixed solution (Figure 4). The calculated $\Delta\Delta G°_{37,competition}$ was lower for Na$^+$ compared to Rb$^+$ and Cs$^+$ for those duplexes. A metal ion with a lower $\Delta\Delta G°_{37,competition}$ corresponds to a metal ion that has a greater influence on secondary structure stability when in a solution with another metal ion. The most stabilizing alkali metal ion, Li$^+$, appeared to influence stability to the same extent as Na$^+$ when in a 1:1 mixed solution. These findings were surprising considering Li$^+$ has been shown to have a higher affinity for the ion atmosphere compared to Na$^+$.[36,45] Both K$^+$ and Na$^+$ were shown to have relatively the same affinity for the ion atmosphere. These findings were contradictory to recent studies that suggested K$^+$ aggregates around the phosphate backbone more so than Na$^+$.[110] One may assume that increased aggregation would lead to increased stability; however, that association may not be the case here.

Improved Predictive Capabilities. Because no studies exist that account for differences in the RNA duplex stability from mixed monovalent cations in solution, a correction factor is needed to account for the presence of more than one alkali metal chloride in a solution. This was the focus of the work presented here that led to the development of eq 6. An

example calculation for using eq 6 is shown below for the 5'-GUAAUAUUAC-3' duplex. The predicted $\Delta G°_{37}$ using the standard NN model in 1.0 M NaCl is −7.90 kcal/mol and will be used to predict the stability of the 5'-GUAAUAUUAC-3' duplex in the 3:1 RbCl/NaCl solution:

$$\Delta G°_{37} \text{ (3:1 RbCl/NaCl)}$$
$$= \Delta G°_{37} \text{ (1.0 M NaCl)} + 0.777 (R_{i,RbCl}) - 0.411$$
$$([RbCl]) - 0.513 (f_{GC}) - 0.782 ([NaCl]) \tag{7}$$

$$\Delta G°_{37} \text{ (3:1 RbCl/NaCl)}$$
$$= -7.90 \text{ kcal/mol} + 0.777 (1.64 \text{ Å}) - 0.411 (0.750 \text{ M})$$
$$- 0.513 (0.20) - 0.782 (0.250 \text{ M}) \tag{8}$$

$$\Delta G°_{37} \text{ (3:1 RbCl/NaCl)} = -7.23 \text{ kcal/mol} \tag{9}$$

The experimental $\Delta G°_{37}$ reported for the 5'-GUAAUAUUAC-3' duplex in 3:1 RbCl/NaCl was −7.17 kcal/mol. The difference between experimental and predicted $\Delta G°_{37}$ using eq 6 is 0.06 kcal/mol. When the 1.0 M NaCl standard NN model is used, the difference between experimental and predicted $\Delta G°_{37}$ is 0.67 kcal/mol. This is a 91% improvement in predictive capabilities for the 5'-GUAAUAUUAC-3' duplex in 3:1 RbCl/NaCl. Other comparisons can be found in the Supporting Information (Table S7).

Implementation with Existing Studies. Most experiments concerned with counting the ions in the ion atmosphere have not considered their impact on the stability of nucleic acids in mixed ion solutions.[36,39−41] Many of those studies have shown conflicting results regarding the preferential occupancy of the ion atmosphere.[13,40,46,110,115,116] Regardless, these studies have provided benchmarks for electrostatic association calculations of metal ions around nucleic acids. The study presented here has shown measurable differences in $\Delta G°_{37}$ for nucleic acids that are dependent on the fraction of GC pairs in an RNA duplex, the identity of alkali metal ions in the solution, and the concentration at which those metal chlorides are mixed. Additionally, the identity of a monovalent metal ion associated with a nucleic acid sample directly impacts its stability in solution. This was seen in mixed ion solutions, where some ions may preferentially occupy the area around the nucleic acid sample. Comparing this to other studies, the findings of an atomistic molecular dynamics simulation study with intrinsically disordered proteins and metal ions suggest that the stability of the protein depends on intrapeptide and peptide−water hydrogen bonds coupled with the heterogeneity of hydration water around the peptide in the presence of various ions.[118] It is likely that similar interactions are involved with nucleic acids in ion solutions, but more experiments are needed to confirm. A myriad of variables need to be considered when performing benchtop or computational studies involving nucleic acids and metal ions. Some of these variables include ion size, dielectric constants, electrostatics of nucleic acids, and the length of nucleic acids. Thorough consideration of each variable should result in improved predictive capabilities for nucleic acid stability in solutions containing more than one monovalent ion. The correction factor presented here could assist in these calculations.

■ ASSOCIATED CONTENT

ⓢ Supporting Information

The Supporting Information is available free of charge at https://pubs.acs.org/doi/10.1021/acsomega.3c07563.

> Supporting methods, supporting results, thermodynamic data and comparisons; example normalized optical melting curves for DNA and RNA duplexes; enthalpy change ($\Delta H°$) for duplex formation in various alkali metal chloride buffers; updated coefficients calculated in the leave-one-out (LOO) analysis; thermodynamics of DNA duplex formation in various 1.0 M alkali metal chlorides; dielectric constants for salt solutions of various concentrations (PDF)

Special Issue Paper

Published as part of *ACS Omega* virtual special issue "Nucleic Acids: A 70th Anniversary Celebration of DNA".

■ AUTHOR INFORMATION

Corresponding Author

Brent M. Znosko − *Department of Chemistry, Saint Louis University, Saint Louis, Missouri 63103, United States;* ⓞ orcid.org/0000-0002-6823-6218; Phone: (314) 977-8567; Email: brent.znosko@slu.edu; Fax: (314) 977-2521

Authors

Sebastian J. Arteaga − *Department of Chemistry, Saint Louis University, Saint Louis, Missouri 63103, United States;* ⓞ orcid.org/0000-0001-7641-7919

Bruce J. Dolenz − *Department of Chemistry, Saint Louis University, Saint Louis, Missouri 63103, United States*

Complete contact information is available at:
https://pubs.acs.org/10.1021/acsomega.3c07563

Notes

The authors declare no competing financial interest.

■ ACKNOWLEDGMENTS

■ REFERENCES

(1) Woese, C. R.; Pace, N. R. *Probing RNA Structure, Function, and History by Comparative Analysis*; Cold Spring Harbor Laboratory Press: Plainview, NY, 1993.

(2) Le Vay, K.; Salibi, E.; Song, E. Y.; Mutschler, H. Nucleic acid catalysis under potential prebiotic conditions. *Chem. - Asian J.* **2020**, *15* (2), 214−230.

(3) Wang, B. The RNA i-motif in the primordial RNA world. *Origins Life Evol. Biospheres* **2019**, *49* (1−2), 105−109.

(4) Kua, J.; Bada, J. L. Primordial ocean chemistry and its compatibility with the RNA world. *Origins Life Evol. Biospheres* **2011**, *41* (6), 553−558.

(5) Martin, W.; Baross, J.; Kelley, D.; Russell, M. J. Hydrothermal vents and the origin of life. *Nat. Rev. Microbiol.* **2008**, *6* (11), 805−814.

(6) Pan, T.; Long, D. M.; Uhlenbeck, O. C. *Divalent Metal Ions in RNA Folding and Catalysis*; Cold Spring Harbor Laboratory Press: Plainview, N.Y., 1993.

(7) Matreux, T.; Le Vay, K.; Schmid, A.; Aikkila, P.; Belohlavek, L.; Caliskanoglu, A. Z.; Salibi, E.; Kuhnlein, A.; Springsklee, C.; Scheu, B.; Dingwell, D. B.; Braun, D.; Mutschler, H.; Mast, C. B. Heat flows in rock cracks naturally optimize salt compositions for ribozymes. *Nat. Chem.* **2021**, *13* (11), 1038−1045.

(8) Mariani, A.; Bonfio, C.; Johnson, C. M.; Sutherland, J. D. pH-driven RNA strand separation under prebiotically plausible conditions. *Biochemistry* **2018**, *57* (45), 6382−6386.

(9) Misra, V. K.; Draper, D. E. The linkage between magnesium binding and RNA folding. *J. Mol. Biol.* **2002**, *317* (4), 507−521.

(10) Takamoto, K.; Das, R.; He, Q.; Doniach, S.; Brenowitz, M.; Herschlag, D.; Chance, M. R. Principles of RNA compaction: Insights from the equilibrium folding pathway of the P4-P6 RNA domain in monovalent cations. *J. Mol. Biol.* **2004**, *343* (5), 1195−1206.

(11) Ogrizek, M.; Konc, J.; Bren, U.; Hodoscek, M.; Janezic, D. Role of magnesium ions in the reaction mechanism at the interface between Tm1631 protein and its DNA ligand. *Chem. Cent. J.* **2016**, *10* (1), No. 41.

(12) Ren, A.; Kosutic, M.; Rajashankar, K. R.; Frener, M.; Santner, T.; Westhof, E.; Micura, R.; Patel, D. J. In-line alignment and Mg^{2+} coordination at the cleavage site of the *env22* twister ribozyme. *Nat. Commun.* **2014**, *5* (1), No. 5534.

(13) Urbanke, C.; Romer, R.; Maass, G. Tertiary structure of tRNA^{Phe} (yeast): Kinetics and electrostatic repulsion. *Eur. J. Biochem.* **1975**, *55* (2), 439−444.

(14) Shiman, R.; Draper, D. E. Stabilization of RNA tertiary structure by monovalent cations. *J. Mol. Biol.* **2000**, *302* (1), 79−91.

(15) Lambert, D.; Leipply, D.; Shiman, R.; Draper, D. E. The influence of monovalent cation size on the stability of RNA tertiary structures. *J. Mol. Biol.* **2009**, *390* (4), 791−804.

(16) Adams, M. S.; Znosko, B. M. Thermodynamic characterization and nearest neighbor parameters for RNA duplexes under molecular crowding conditions. *Nucleic Acids Res.* **2019**, *47* (7), 3658−3666.

(17) Kilburn, D.; Roh, J. H.; Behrouzi, R.; Briber, R. M.; Woodson, S. A. Crowders perturb the entropy of RNA energy landscapes to favor folding. *J. Am. Chem. Soc.* **2013**, *135* (27), 10055−10063.

(18) Ghosh, S.; Takahashi, S.; Banerjee, D.; Ohyama, T.; Endoh, T.; Tateishi-Karimata, H.; Sugimoto, N. Nearest-neighbor parameters for the prediction of RNA duplex stability in diverse in vitro and cellular-like crowding conditions. *Nucleic Acids Res.* **2023**, *51* (9), 4101−4111.

(19) Akabayov, B.; Akabayov, S. R.; Lee, S. J.; Wagner, G.; Richardson, C. C. Impact of macromolecular crowding on DNA replication. *Nat. Commun.* **2013**, *4* (1), No. 1615.

(20) Barber, R.; Noble, M. Binding of alkali metal ions to polynucleotides. *Biochim. Biophys. Acta, Nucleic Acids Protein Synth.* **1966**, *123* (1), 205−207.

(21) Owczarzy, R.; You, Y.; Moreira, B. G.; Manthey, J. A.; Huang, L.; Behlke, M. A.; Walder, J. A. Effects of sodium ions on DNA duplex oligomers: Improved predictions of melting temperatures. *Biochemistry* **2004**, *43* (12), 3537−3554.

(22) Owczarzy, R.; Moreira, B. G.; You, Y.; Behlke, M. A.; Walder, J. A. Predicting stability of DNA duplexes in solutions containing magnesium and monovalent cations. *Biochemistry* **2008**, *47* (19), 5336−5353.

(23) Chen, Z.; Znosko, B. M. Effect of sodium ions on RNA duplex stability. *Biochemistry* **2013**, *52* (42), 7477−7485.

(24) Manning, G. S. On the application of polyelectrolyte "limiting laws" to the helix-coil transition of DNA. II. The effect of Mg^{2+} counterions. *Biopolymers* **1972**, *11* (5), 951−955.

(25) Huguet, J. M.; Ribezzi-Crivellari, M.; Bizarro, C. V.; Ritort, F. Derivation of nearest-neighbor DNA parameters in magnesium from single molecule experiments. *Nucleic Acids Res.* **2017**, *45* (22), 12921−12931.

(26) Nixon, P. L.; Theimer, C. A.; Giedroc, D. P. Thermodynamics of stabilization of RNA pseudoknots by cobalt(III) hexaammine. *Biopolymers* **1999**, *50* (4), 443−458.

(27) Heilman-Miller, S. L.; Thirumalai, D.; Woodson, S. A. Role of counterion condensation in folding of the *Tetrahymena* ribozyme. I. Equilibrium stabilization by cations. *J. Mol. Biol.* **2001**, *306* (5), 1157−1166.

(28) Dumas, L.; Herviou, P.; Dassi, E.; Cammas, A.; Millevoi, S. G-Quadruplexes in RNA biology: Recent advances and future directions. *Trends Biochem. Sci.* **2021**, *46* (4), 270−283.

(29) Draper, D. E. A guide to ions and RNA structure. *RNA* **2004**, *10* (3), 335−343.

(30) Dallas, A.; Vlassov, A. V.; Kazakov, S. A. *Principles of Nucleic Acid Cleavage by Metal Ions*; Springer: Santa Cruz, CA, 2004; Vol. 13.

(31) Manning, G. S. Limiting laws and counterion condensation in polyelectrolyte solutions I. Colligative properties. *J. Chem. Phys.* **1969**, *51* (3), 924−933.

(32) Lipfert, J.; Doniach, S.; Das, R.; Herschlag, D. Understanding nucleic acid-ion interactions. *Annu. Rev. Biochem.* **2014**, *83* (1), 813−841.

(33) Draper, D. E. RNA folding: Thermodynamic and molecular descriptions of the roles of ions. *Biophys. J.* **2008**, *95* (12), 5489−5495.

(34) Giedroc, D. P.; Grossoehme, N. E. Nucleic Acid-Metal Ion Interactions. In *Metal Ions and the Thermodynamics of RNA Folding*; Royal Society of Chemistry: Cambridge, UK, 2009; Chapter 6.

(35) Weitzner, S. E.; Pham, T. A.; Orme, C. A.; Qiu, S. R.; Wood, B. C. Beyond thermodynamics: Assessing the dynamical softness of hydrated ions from first principles. *J. Phys. Chem. Lett.* **2021**, *12* (49), 11980−11986.

(36) Bai, Y.; Greenfeld, M.; Travers, K. J.; Chu, V. B.; Lipfert, J.; Doniach, S.; Herschlag, D. Quantitative and comprehensive decomposition of the ion atmosphere around nucleic acids. *J. Am. Chem. Soc.* **2007**, *129* (48), 14981−14988.

(37) Greenfeld, M.; Herschlag, D. Probing Nucleic Acid−Ion Interactions with Buffer Exchange-Atomic Emission Spectroscopy. In *Methods in Enzymology*; Academic Press, 2009; Chapter 18, Vol. *469*, pp 375−389.

(38) Yu, B.; Iwahara, J. Experimental approaches for investigating ion atmospheres around nucleic acids and proteins. *Comput. Struct. Biotechnol. J.* **2021**, *19*, 2279−2285.

(39) Gebala, M.; Giambaşu, G. M.; Lipfert, J.; Bisaria, N.; Bonilla, S.; Li, G.; York, D. M.; Herschlag, D. Cation−anion interactions within the nucleic acid ion atmosphere revealed by ion counting. *J. Am. Chem. Soc.* **2015**, *137* (46), 14705−14715.

(40) Gebala, M.; Bonilla, S.; Bisaria, N.; Herschlag, D. Does cation size affect occupancy and electrostatic screening of the nucleic acid ion atmosphere? *J. Am. Chem. Soc.* **2016**, *138* (34), 10925−10934.

(41) Gebala, M.; Herschlag, D. Quantitative studies of an RNA duplex electrostatics by ion counting. *Biophys. J.* **2019**, *117* (6), 1116−1124.

(42) Shahi, M. R.; Bagheri, S. The effect of metal alkali cations on the properties of hydrogen bonds in tautomeric forms of adenine - guanine mismatch. *J. Mol. Graph. Model.* **2020**, *100*, No. 107705.

(43) Rodgers, M. T.; Armentrout, P. B. Noncovalent interactions of nucleic acid bases (uracil, thymine, and adenine) with alkali metal ions. Threshold collision-induced dissociation and theoretical studies. *J. Am. Chem. Soc.* **2000**, *122* (35), 8548−8558.

(44) Bhai, S.; Ganguly, B. Role of backbones on the interaction of metal ions with deoxyribonucleic acid and peptide nucleic acid: A DFT study. *J. Mol. Graph. Model.* **2019**, *93*, No. 107445.

(45) Savelyev, A.; MacKerell, A. D., Jr. Competition among Li^+, Na^+, K^+, and Rb^+ monovalent ions for DNA in molecular dynamics simulations using the additive CHARMM36 and Drude polarizable force fields. *J. Phys. Chem. B* **2015**, *119* (12), 4428−4440.

(46) Giambaşu, G. M.; Gebala, M. K.; Panteva, M. T.; Luchko, T.; Case, D. A.; York, D. M. Competitive interaction of monovalent cations with DNA from 3D-RISM. *Nucleic Acids Res.* **2015**, *43* (17), 8405−8415.

(47) Savelyev, A.; MacKerell, A. D., Jr. Differential impact of the monovalent ions Li^+, Na^+, K^+, and Rb^+ on DNA conformational properties. *J. Phys. Chem. Lett.* **2015**, *6* (1), 212−216.

(48) Sun, S.; Karki, C.; Xie, Y.; Xian, Y.; Guo, W.; Gao, B. Z.; Li, L. Hybrid method for representing ions in implicit solvation calculations. *Comput. Struct. Biotechnol. J.* **2021**, *19*, 801−811.

(49) Wang, K.; Yu, Y.-X.; Gao, G.-H.; Luo, G.-S. Preferential interaction between DNA and small ions in mixed-size counterion systems: Monte Carlo simulation and density functional study. *J. Chem. Phys.* **2007**, *126* (13), No. 135102.

(50) Pinnavaia, T. J.; Marshall, C. L.; Mettler, C. M.; Fisk, C. L.; Miles, H. T.; Becker, E. D. Alkali metal ion specificity in the solution ordering of a nucleotide, 5′-guanosine monophosphate. *J. Am. Chem. Soc.* **1978**, *100* (11), 3625−3627.

(51) Nakano, S.-i.; Fujimoto, M.; Hara, H.; Sugimoto, N. Nucleic acid duplex stability: Influence of base composition on cation effects. *Nucleic Acids Res.* **1999**, *27* (14), 2957−2965.

(52) Tan, Z.-J.; Chen, S.-J. Nucleic acid helix stability: Effects of salt concentration, cation valence and size, and chain length. *Biophys. J.* **2006**, *90* (4), 1175−1190.

(53) Bizarro, C. V.; Alemany, A.; Ritort, F. Non-specific binding of Na$^+$ and Mg^{2+} to RNA determined by force spectroscopy methods. *Nucleic Acids Res.* **2012**, *40* (14), 6922−6935.

(54) Trachman, R. J., III; Draper, D. E. Divalent ion competition reveals reorganization of an RNA ion atmosphere upon folding. *Nucleic Acids Res.* **2017**, *45* (8), 4733−4742.

(55) Tan, Z.-J.; Chen, S.-J. RNA helix stability in mixed Na$^+$/Mg^{2+} solution. *Biophys. J.* **2007**, *92* (10), 3615−3632.

(56) Leamy, K. A.; Assmann, S. M.; Mathews, D. H.; Bevilacqua, P. C. Bridging the gap between in vitro and in vivo RNA folding. *Q. Rev. Biophys.* **2016**, *49*, No. e10.

(57) Rakova, N.; Kitada, K.; Lerchl, K.; Dahlmann, A.; Birukov, A.; Daub, S.; Kopp, C.; Pedchenko, T.; Zhang, Y.; Beck, L.; Johannes, B.; Marton, A.; Muller, D. N.; Rauh, M.; Luft, F. C.; Titze, J. Increased salt consumption induces body water conservation and decreases fluid intake. *J. Clin. Invest.* **2017**, *127* (5), 1932−1943.

(58) Hodgkin, A. L.; Huxley, A. F. A quantitative description of membrane current and its application to conduction and excitation in nerve. *J. Physiol.* **1952**, *117* (4), 500−544.

(59) Clausen, T. Na$^+$-K$^+$ pump regulation and skeletal muscle contractility. *Physiol. Rev.* **2003**, *83* (4), 1269−1324.

(60) Cobb, M.; Pacitti, D. The importance of sodium restrictions in chronic kidney disease. *J. Renal Nutr.* **2018**, *28* (5), e37−e40.

(61) Tavakol, E.; Jakli, B.; Cakmak, I.; Dittert, K.; Senbayram, M. Optimization of potassium supply under osmotic stress mitigates oxidative damage in barley. *Plants* **2022**, *11* (1), 55.

(62) Cochrane, T. T.; Cochrane, T. A. The vital role of potassium in the osmotic mechanism of stomata aperture modulation and its link with potassium deficiency. *Plant Signal. Behav.* **2009**, *4* (3), 240−243.

(63) Haddy, F. J.; Vanhoutte, P. M.; Feletou, M. Role of potassium in regulating blood flow and blood pressure. *Am. J. Physiol.: Regul., Integr. Comp. Physiol.* **2006**, *290* (3), R546−R552.

(64) Chatterjee, R.; Yeh, H. C.; Edelman, D.; Brancati, F. Potassium and risk of type 2 diabetes. *Expert. Rev. Endocrinol. Metab.* **2011**, *6* (5), 665−672.

(65) Stone, M. S.; Martyn, L.; Weaver, C. M. Potassium intake, bioavailability, hypertension, and glucose control. *Nutrients* **2016**, *8* (7), 444.

(66) Udensi, U. K.; Tchounwou, P. B. Potassium homeostasis, oxidative stress, and human disease. *Int. J. Clin. Exp. Physiol.* **2017**, *4* (3), 111−122.

(67) Nierenberg, A. A.; Agustini, B.; Kohler-Forsberg, O.; Cusin, C.; Katz, D.; Sylvia, L. G.; Peters, A.; Berk, M. Diagnosis and treatment of bipolar disorder: A review. *JAMA* **2023**, *330* (14), 1370−1380.

(68) Zhuo, C.; Hu, S.; Chen, G.; Yang, L.; Cai, Z.; Tian, H.; Jiang, D.; Chen, C.; Wang, L.; Ma, X.; Li, R. Low-dose lithium adjunct to atypical antipsychotic treatment nearly improved cognitive impairment, deteriorated the gray-matter volume, and decreased the interleukin-6 level in drug-naive patients with first schizophrenia symptoms: A follow-up pilot study. *Schizophrenia* **2023**, *9* (1), No. 71.

(69) Matsuoka, R.; Fudim, R.; Jung, S.; Zhang, C.; Bazzone, A.; Chatzikyriakidou, Y.; Robinson, C. V.; Nomura, N.; Iwata, S.; Landreh, M.; Orellana, L.; Beckstein, O.; Drew, D. Structure, mechanism and lipid-mediated remodeling of the mammalian Na$^+$/H$^+$ exchanger NHA2. *Nat. Struct. Mol. Biol.* **2022**, *29* (2), 108−120.

(70) Quintero, J. M.; Molina, R.; Fournier, J. M.; Benlloch, M.; Ramos, J. Glucose-induced activation of rubidium transport and water flux in sunflower root systems. *J. Exp. Bot.* **2001**, *52* (354), 99−104.

(71) Meltzer, H. L.; Lieberman, K. W.; Shelley, E. M.; Stallone, F.; Fieve, R. R. Metabolism of naturally occurring Rb in the human: The constancy of urinary Rb-K. *Biochem. Med.* **1973**, *7* (2), 218−225.

(72) Chatal, J. F.; Rouzet, F.; Haddad, F.; Bourdeau, C.; Mathieu, C.; Le Guludec, D. Story of rubidium-82 and advantages for myocardial perfusion PET imaging. *Front. Med.* **2015**, *2*, No. 65.

(73) Ahmadi, A.; Klein, R.; Lewin, H. C.; Beanlands, R. S. B.; deKemp, R. A. Rubidium-82 generator yield and efficiency for PET perfusion imaging: Comparison of two clinical systems. *J. Nucl. Cardiol.* **2020**, *27* (5), 1728−1738.

(74) Yamagata, N. The concentration of common cesium and rubidium in human body. *J. Radiat. Res.* **1962**, *3* (1), 9−30.

(75) Kernan, R. P.; McDermott, M. Rubidium influx into rat skeletal muscles in relation to electrical activity. *J. Physiol.* **1973**, *233* (2), 363−374.

(76) Mülhardt, C.; Beese, E. W. Cloning DNA fragments. In *Molecular Biology and Genomics*; Mülhardt, C.; Beese, E. W., Eds.; Academic Press: Burlington, 2007; pp 105−129.

(77) Collins, D. A.; Kalyuzhnaya, M. G. Navigating methane metabolism: Enzymes, compartments, and networks. In *Methods in Enzymology*; Armstrong, F., Ed.; Academic Press, 2018; Chapter 14, Vol. *613*, pp 349−383.

(78) Green, R.; Rogers, E. J. Transformation of chemically competent *E. coli. Methods Enzymol.* **2013**, *529*, 329−336.

(79) Avery, S. V.; Codd, G. A.; Gadd, G. M. Replacement of cellular potassium by caesium in *Chlorella emersonii*: Differential sensitivity of photoautotrophic and chemoheterotrophic growth. *Microbiology* **1992**, *138* (1), 69−76.

(80) Guerin, M.; Wallon, G. The reversible replacement of internal potassium by caesium in isolated turtle heart. *J. Physiol.* **1979**, *293* (1), 525−537.

(81) Xia, T.; SantaLucia, J., Jr.; Burkard, M. E.; Kierzek, R.; Schroeder, S. J.; Jiao, X.; Cox, C.; Turner, D. H. Thermodynamic parameters for an expanded nearest-neighbor model for formation of RNA duplexes with Watson-Crick base pairs. *Biochemistry* **1998**, *37* (42), 14719−14735.

(82) Williams, A. P.; Longfellow, C. E.; Freier, S. M.; Kierzek, R.; Turner, D. H. Laser temperature-jump, spectroscopic, and thermodynamic study of salt effects on duplex formation by dGCATGC. *Biochemistry* **1989**, *28* (10), 4283−4291.

(83) Breslauer, K. J.; Frank, R.; Blöcker, H.; Marky, L. A. Predicting DNA duplex stability from the base sequence. *Proc. Natl. Acad. Sci. U.S.A.* **1986**, *83* (11), 3746−3750.

(84) Reuter, J. S.; Mathews, D. H. RNAstructure: Software for RNA secondary structure prediction and analysis. *BMC Bioinf.* **2010**, *11* (1), No. 129.

(85) Bellaousov, S.; Reuter, J. S.; Seetin, M. G.; Mathews, D. H. RNAstructure: Web servers for RNA secondary structure prediction and analysis. *Nucleic Acids Res.* **2013**, *41*, W471−W474.

(86) Mathews, D. H. Using an RNA secondary structure partition function to determine confidence in base pairs predicted by free energy minimization. *RNA* **2004**, *10* (8), 1178−1190.

(87) Spasic, A.; Berger, K. D.; Chen, J. L.; Seetin, M. G.; Turner, D. H.; Mathews, D. H. Improving RNA nearest neighbor parameters for helices by going beyond the two-state model. *Nucleic Acids Res.* **2018**, *46* (10), 4883−4892.

(88) Wright, D. J.; Rice, J. L.; Yanker, D. M.; Znosko, B. M. Nearest neighbor parameters for inosine·uridine pairs in RNA duplexes. *Biochemistry* **2007**, *46* (15), 4625−4634.

(89) Freier, S. M.; Kierzek, R.; Jaeger, J. A.; Sugimoto, N.; Caruthers, M. H.; Neilson, T.; Turner, D. H. Improved free-energy parameters for predictions of RNA duplex stability. *Proc. Natl. Acad. Sci. U.S.A.* **1986**, *83* (24), 9373−9377.

(90) He, L.; Kierzek, R.; SantaLucia, J., Jr.; Walter, A. E.; Turner, D. H. Nearest-neighbor parameters for G·U mismatches: $^{5'\mathrm{GU3'}}_{3'\mathrm{UG5'}}$ is destabilizing in the contexts $^{\mathrm{CGUG}}_{\mathrm{GUGC}}$, $^{\mathrm{UGUA}}_{\mathrm{AUGU}}$, and $^{\mathrm{AGUU}}_{\mathrm{UUGA}}$ but stabilizing in $^{\mathrm{GGUC}}_{\mathrm{CUGG}}$. *Biochemistry* **1991**, *30* (46), 11124−11132.

(91) SantaLucia, J., Jr.; Allawi, H. T.; Seneviratne, P. A. Improved nearest-neighbor parameters for predicting DNA duplex stability. *Biochemistry* **1996**, *35* (11), 3555−3562.

(92) McDowell, J. A.; Turner, D. H. Investigation of the structural basis for thermodynamic stabilities of tandem GU mismatches: Solution structure of (rGAGGUCUC)$_2$ by two-dimensional NMR and simulated annealing. *Biochemistry* **1996**, *35* (45), 14077−14089.

(93) Schroeder, S. J.; Turner, D. H. Optical Melting Measurements of Nucleic Acid Thermodynamics. In *Methods in Enzymology*; Academic Press, 2009; Vol. *468*, pp 371−387.

(94) Borer, P. N.; Dengler, B.; Tinoco, I., Jr.; Uhlenbeck, O. C. Stability of ribonucleic acid double-stranded helices. *J. Mol. Biol.* **1974**, *86* (4), 843−853.

(95) Zuber, J.; Schroeder, S. J.; Sun, H.; Turner, D. H.; Mathews, D. H. Nearest neighbor rules for RNA helix folding thermodynamics: Improved end effects. *Nucleic Acids Res.* **2022**, *50* (9), 5251−5262.

(96) Arteaga, S. J.; Adams, M. S.; Meyer, N. L.; Richardson, K. E.; Hoener, S.; Znosko, B. M. Thermodynamic determination of RNA duplex stability in magnesium solutions. *Biophys. J.* **2023**, *122* (3), 565−576.

(97) Chin, K.; Sharp, K. A.; Honig, B.; Pyle, A. M. Calculating the electrostatic properties of RNA provides new insights into molecular interactions and function. *Nat. Struct. Biol.* **1999**, *6* (11), 1055−1061.

(98) Xi, K.; Wang, F. H.; Xiong, G.; Zhang, Z. L.; Tan, Z. J. Competitive binding of Mg^{2+} and Na^+ ions to nucleic acids: From helices to tertiary structures. *Biophys. J.* **2018**, *114* (8), 1776−1790.

(99) Pan, F.; Roland, C.; Sagui, C. Ion distributions around left- and right-handed DNA and RNA duplexes: A comparative study. *Nucleic Acids Res.* **2014**, *42* (22), 13981−13996.

(100) Chamberlin, M. J.; Patterson, D. L. Physical and chemical characterization of the ordered complexes formed between poly-inosinic acid, polycytidylic acid and their deoxyribo-analogues. *J. Mol. Biol.* **1965**, *12* (2), 410−428.

(101) Roberts, R. W.; Crothers, D. M. Stability and properties of double and triple helices: Dramatic effects of RNA or DNA backbone composition. *Science* **1992**, *258* (5087), 1463−1466.

(102) Hung, S. H.; Yu, Q.; Gray, D. M.; Ratliff, R. L. Evidence from CD spectra that d(purine)·r(pyrimidine) and r(purine)·d-(pyrimidine) hybrids are in different structural classes. *Nucleic Acids Res.* **1994**, *22* (20), 4326−4334.

(103) Lesnik, E. A.; Freier, S. M. Relative thermodynamic stability of DNA, RNA, and DNA:RNA hybrid duplexes: Relationship with base composition and structure. *Biochemistry* **1995**, *34* (34), 10807−10815.

(104) Rauzan, B.; McMichael, E.; Cave, R.; Sevcik, L. R.; Ostrosky, K.; Whitman, E.; Stegemann, R.; Sinclair, A. L.; Serra, M. J.; Deckert, A. A. Kinetics and thermodynamics of DNA, RNA, and hybrid duplex formation. *Biochemistry* **2013**, *52* (5), 765−772.

(105) Sharp, K. Entropy-enthalpy compensation: Fact or artifact? *Protein Sci.* **2001**, *10* (3), 661−667.

(106) Krug, R. R.; Hunter, W. G.; Grieger, R. A. Enthalpy-entropy compensation. 1. Some fundamental statistical problems associated with the analysis of van't Hoff and Arrhenius data. *J. Phys. Chem. A* **1976**, *80* (21), 2335−2341.

(107) Majikes, J. M.; Zwolak, M.; Liddle, J. A. Best practice for improved accuracy: A critical reassessment of van't Hoff analysis of melt curves. *Biophys. J.* **2022**, *121* (11), 1986−2001.

(108) Mähler, J.; Persson, I. A study of the hydration of the alkali metal ions in aqueous solution. *Inorg. Chem.* **2012**, *51* (1), 425−438.

(109) Wanrooij, P. H.; Uhler, J. P.; Simonsson, T.; Falkenberg, M.; Gustafsson, C. M. G-quadruplex structures in RNA stimulate mitochondrial transcription termination and primer formation. *Proc. Natl. Acad. Sci. U.S.A.* **2010**, *107* (37), 16072−16077.

(110) Henning-Knechtel, A.; Thirumalai, D.; Kirmizialtin, S. Differences in ion-RNA binding modes due to charge density variations explain the stability of RNA in monovalent salts. *Sci. Adv.* **2022**, *8* (29), No. eabo1190.

(111) Dilip, H. N.; Chakraborty, D. Hydrophilicity of the hydrophobic group: Effect of cosolvents and ions. *J. Mol. Liq.* **2019**, *280*, 389−398.

(112) Bloomfield, V. A.; Crothers, D. M.; Tinoco, I., Jr. *Nucleic Acids: Structure, Properties, and Functions*; University Science Books: Sausalito, CA, 2000.

(113) Xu, H. T.; Zhang, N.; Li, M. R.; Zhang, F. S. Anion effect of Cl^-, I^-, and F^- on counterions condensation within nucleic acid ion atmosphere. *J. Mol. Liq.* **2021**, *332*, No. 115899, DOI: 10.1016/j.molliq.2021.115899.

(114) Ma, C. Y.; Pezzotti, S.; Schwaab, G.; Gebala, M.; Herschlag, D.; Havenith, M. Cation enrichment in the ion atmosphere is promoted by local hydration of DNA. *Phys. Chem. Chem. Phys.* **2021**, *23* (40), 23203−23213.

(115) Ross, P. D.; Scruggs, R. L. Electrophoresis of DNA. II. Specific interactions of univalent and divalent cations with DNA. *Biopolymers* **1964**, *2* (1), 79−89.

(116) Yu, B. H.; Bien, K. G.; Wang, T. Z.; Iwahara, J. Diffusion NMR-based comparison of electrostatic influences of DNA on various monovalent cations. *Biophys. J.* **2022**, *121* (18), 3562−3570.

(117) Frank-Kamenetskii, M. D. Simplification of the empirical relationship between melting temperature of DNA, its GC content and concentration of sodium ions in solution. *Biopolymers* **1971**, *10* (12), 2623−2624.

(118) Singh, O.; Kumar Das, B.; Chakraborty, D. Influence of ion specificity and concentration on the conformational transition of intrinsically disordered sheep prion peptide. *ChemPhysChem* **2022**, *23* (16), No. e202200211.